OPTICAL MEMS IMAGE ENHANCEMENT WITH SPARSE SIGNAL REPRESENTATION

Ganchi Zhang, Li Li, Vladimir Stanković, Lina Stanković, Deepak Uttamchandani

Dept. Electronic and Electrical Engineering, University of Strathclyde, Glasgow, UK

ABSTRACT

This paper describes a complete low-complexity imaging system based on a single MEMS scanning mirror and a single photodetector, together with customized image enhancement algorithms based on sparse signal representation. Due to very low complexity of our developped optical set-up for image acquisition, resulting images suffer visible artifacts. We propose an iterative denoising-deblurring algorithm for image enhancement, which offers significant improvement over wavelet denoising with soft-thresholding. Several image enhancement algorithms are compared using the blind image quality indices (BIQI) as well as visual experience.

Index Terms— image enhancement, sparse representation

1. INTRODUCTION

Recent trends in miniaturization are increasingly motivating multidisciplinary research into manufacturing technologies, optics, micro- and nano-technology and signal/image processing in order to manufacture cheap image acquisition equipment with low power consumption. Current advances indicate that while it is possible via micro-electromechanical systems (MEMS), nano-technology and optics, to manufacture such miniature devices, the price to pay is poor image quality. This motivates the need for powerful image processing restoration methods.

This paper builds on the low-cost and miniature optical imaging system proposed in [1], with only a single MEMS scanning mirror and a single photo-detector. The penalty of the cheap and extremely low cost acquisition complexity of the system was a poor imaging performance. To enhance the acquired images, wavelet denoising with soft thresholding [11] together with bilinear interpolation were used providing some improvements, but visual results presented in [1] still indicate much room for improvement.

Therefore, to enhance the resulting image, we propose two major improvements to the system of [1]. First, the image-capture architecture is improved via smaller pinhole and better focussing optics which resulted in higher SNR at the photodetector. Secondly, we replace the wavelet denoising with soft thresholding algorithm by an iterative image denoising-deblurring algorithm that jointly removes noise and blur in the experimentally generated image. The proposed algorithm exploits sparsity of the image. It is based on learning the best "dictionary" to sparsely represent noisy image data using K-SVD [2] with Orthogonal Matching Pursuit (OMP) [5], and then applying reflexive boundary condition with Tikhonov Regularization [3] for deblurring. The process iterates between denoising and deblurring until a satisfactory condition is met or no further improvement can be noticed.

Additionally, we apply blind image quality indices (BIQI) [6] to objectively assess the quality of the reconstructed images post image processing since there is no original image in this case for classical peak signal-to-noise ratio (PSNR) comparison. We restrict BIQI indexing by taking into account only relevant artifacts: white noise, blur, and fast fading.

The key contribution of the paper is the overall multidisciplinary system design: from the experimental optical setup with a MEMS scanner to image processing. The paper modifies, adapts, and tests several image enhancement tools tailored to the specific nature of our low-complexity imaging experimental set-up. The rest of the paper is organized as follows. Section 2 outlines how we acquire images with our experimental set-up, Section 3 describes the proposed image enhancement algorithm, and the last two sections are dedicated to performance analysis and conclusions.

2. OPTICAL IMAGING SYSTEM

This section describes our experimental optical imaging system (see Fig. 1), that is built on the system proposed in [1].

A single electrical bulb shining on a printed image (object) is used as source generator. Light reflected from the object passes through a system of lenses and a macro-mirror is used to fold the optical path between the MEMS mirror and the object to obtain a compact footprint for the imaging system. The demagnified image is incident on the MEMS scanning mirror of size $2.5\text{x}2.5$ mm^2. The light reflected from the MEMS mirror passes through a pinhole and is incident on the single photo-detector. The focusing optics ensure that the light captured from the object is fully intercepted by the surface of the scanning micromirror as it travels to the pin-

The authors wish to acknowledge support from the University of Strathclyde 2008 Annual Research Prize Award and the Glasgow Research Partnership in Engineering (GRPE). The work is also partly supported by the Electro-Magnetic Remote Sensing (EMRS) Defence Technology Centre established by the UK Ministry of Defence and run by a consortium of SELEX Galileo, Thales UK, Roke Manor Research and Filtronics.

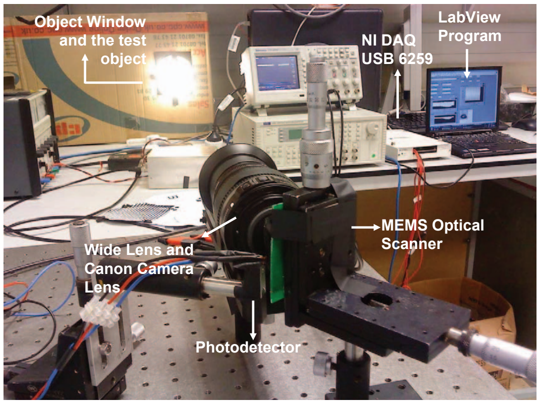

Fig. 1. System setup.

hole. The image that is formed at the plane of the pinhole can be shifted with high precision in the xy-plane by scanning the MEMS mirror in the horizontal and/or vertical direction under electrical control. A National Instruments Digital Acquisition (NI DAQ) module, which contains a microcontroller programmable by a PC, is used to finely adjust the mirror orientation in programmable steps. The same PC is also used to collect readings from the photo-detector's output which is also connected to the NI DAQ module. Different scanning rates were tested and we observed that 90Hz was accepted as the rate that offered the best tradeoff between the acquisition time and performance.

The image acquisition process proceeds as follows. First, we fixed the control voltage on one actuator pair of the micromirror, which controls vertical shift, and changed the voltage on the other pair, which controls horizontal shift, by a fixed voltage step. For each voltage level, the photo-detector sees only one part of the projected image through the pinhole. The reading that corresponds to the accumulated brightness of this area is recorded by the PC. By changing the voltage, the area seen by the detector shifts from left to right. After the entire row is scanned, the voltage on the horizontal actuator is reset and the voltage on the vertical actuator incremented by a voltage step. This corresponds to conventional scanning with a negative scanning raster. To reduce the size of the scanned area we used a pinhole of 50μm in diameter, which differs from 300μm used in [1]. Another difference compared to the system of [1] lies in replacing three biconvex lenses with focal length of 10cm by a digital camera lens, namely Canon EFS 18-55mm, plus a wide-angle lens, namely Fujiyama 0.42xAF digital wide lens. Consequently, the light intensity received by the photodetector is significantly improved, and the field view is increased (due to the wide lens). This way signal-to-noise ratio (SNR) at the photodetector is increased from 4-5dB with the system of [1] to more than 35dB.

As mentioned before, due to the low complexity of the imaging system, the acquired images still suffer a high level of random noise due to measuring equipment. In order to mitigate the effect of noise, for each pixel of the image, we repeat each pixel measurement 100 times, obtaining 100 voltage readings, which are averaged to obtain final pixel values. Some examples of the resulting images are shown in Figs. 3 (a) and 4 (a). The acquired images are then fed to the image enhancement algorithm described next.

3. BLIND IMAGE DENOISING/DEBLURRING

Figs. 3 (a) and 4 (a) indicate that the images suffer from a high level of mainly white noise, due to the non-polarized light source and measurement equipment, and from defocussing blur. In this section we describe the proposed image enhancement algorithm, whose block diagram is depicted in Fig. 2. The core of the algorithm comprises the iterative image denoising method via sparse signal representation [2], and a deblurring technique, applying reflexive boundary condition with Tikhonov Regularization [3].

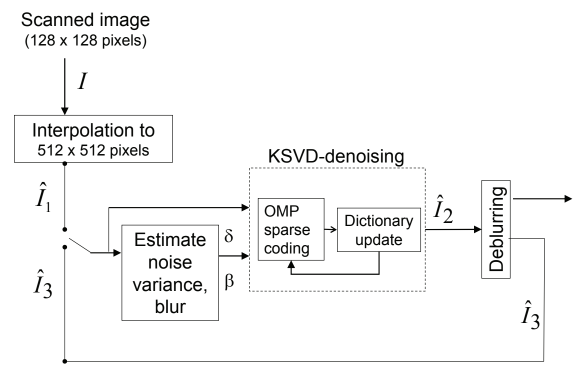

Fig. 2. The proposed algorithm, where the switch is flipped up for the first iteration, and the switch is down for the next remaining iterations.

The proposed algorithm is initialised as follows. The experimental image acquired from the optical imaging system described in Section 2 is first interpolated from their acquired size of 128×128 pixels to the desired size of 512×512 pixels. The next step is the estimation of white noise level σ and blur level β, that can be achieved either heuristically, or using, for example, the methods of [7, 6].

The interpolated image $\hat{I}_1$ together with the two aforementioned noise parameters is then fed to the iterative denoising block comprising OMP-based sparse coding with a dictionary update. Image denoising using sparse image representation is a powerful technique competitive to state-of-the-art denoising methods. The idea is to "learn" the best basis functions or "dictionary" that leads to the sparsest image representation, and denoise the image in the sparsest domain. Several techniques for denoising using sparse image representation have been proposed (see, for example, [2, 8] and references therein). In this paper we follow the state-of-the-art approach of [2], and resort to K-SVD for dictionary learning and OMP for sparse coding via l_0 norm minimization. The process iterates between dictionary adaptation and the sparse coding stage until the error falls below a predetermined threshold. We used the interpolated noisy image $\hat{I}_1$ for training with overlapping patches. Once the error falls below the threshold, the image is recovered by averaging of the overlapping denoised patches.

The denoising step is followed by a deblurring step. A number of deblurring methods were tested, namely (i) Tikhonov image deblurring using the FFT algorithm and the Kronecker decomposition, (ii) the truncated SVD image (tsvd) deblurring using DCT or FFT algorithm, and (iii) blind Tikhonov image deblurring using DCT algorithm (tik-dct) [3]. We observed that for our application the first two algorithms generated worse results than tik-dct. Tik-dct restores the image using a DCT-based Tikhonov filter [4] with the identity matrix as the regularization operator. We used the point spread function for out-of-focus blur.

The process of noise parameter estimation, denoising, and deblurring is repeated until a pre-determined number of iterations is reached. Note that after each denoising-deblurring iteration, noise parameters σ and β, and the number of iterations within the KSVD-denoising block [2] are reduced to account for the improved intermediate image quality.

4. RESULTS

In this section we report our image enhancement results. In order to assess the quality of the denoised-deblurred images and compare results to other techniques, besides subjective visual experience, we use the blind image quality indices (BIQI) of [6]. BIQI is a non-reference image quality indices that assume no knowledge of the distortion affecting the image. The method first classifies images into five difference distortion categories (JPEG, JPEG2000, white Gaussian noise, blur, fast fading), and then assess the quality of the image. BIQI provides a quality index between 0 and 100, with 0 being the best quality and 100 the worst. BIQI are obtained by training and corresponds well to the human visual experience [6]. We modified the original BIQI taking only into account relevant artifacts, due to white Gaussian noise, blur, and fast fading.

Several state-of-the-art denoising and deblurring techniques are compared. The proposed method comprises the K-SVD denoising algorithm with OMP sparse coding and blind Tikhonov image deblurring using DCT algorithm (tik-dct). For comparison, we also test under same conditions the following denoising algorithms: framelet denoising (FD) [9], complex 2D dual-tree DWT (DT-DWT) [10], and wavelet denoising with soft thresholding (WST) [11, 12]; and the following deblurring algorithms: Tikhonov image deblurring using the FFT algorithm and the Kronecker decomposition (tik-fft), and the truncated SVD image deblurring using DCT or FFT algorithm (tsvd-dct).

We present our results for two images (objects comprising capital letters "G", and "R") generated from our optical imaging experimental set-up of Sec. 2.

Table 1. The BIQI results for the six algorithms and the two experimental images.

Algorithm	G	R
Original	88.98	100
FD	50.75	56.16
DT-DWT	58.47	56.25
WST	98.23	95.06
Proposed 1 iter	65.63	74.46
Proposed 2 iter tik-fft	47.38	53.50
Proposed 2 iter tsvd-dct	60.45	66.98
Proposed 2 iter	37.16	24.76

All images obtained by our experimental setup are of size 128×128 pixels. The images are first interpolated using bilinear interpolation to the size of 512×512 pixels, and then the enhancement algorithms are applied as described in Sec. 3.

For the proposed algorithm, we always start with 10 iterations for the K-SVD image denoising, set noise deviation to $\sigma = 15$, and blur level to $\beta = 1.2$, which we found to be best heuristically. In the second iteration after the first deblurring, the blur level was decreased fourfold, noise deviation set to 1, and the number of K-SVD iterations decreased to 5.

Table 1 shows the BIQI results, for all tested denoising algorithms coupled with tik-dct, and where the image acquired from our optical imaging set-up is referred to as "Original". It can be seen from the table that the proposed algorithms significantly improve image quality compared to the experimental output. Also noteworthy is that the WST algorithm used in [1] performs worst for all images. For letters "R" and "G", the proposed algorithm significantly outperforms the other three. "Proposed 2 iter tik-fft (tsvd-dct)" show results of the proposed method, when instead of tik-dct, tik-fft or tsvd-dct is used. It can be seen that tik-dct is the best choice.

The second iteration of the proposed algorithm significantly improves the BIQI. However, we observe no improvement with further iterations. K-SVD alone (without deblurring) gives worse performance (for example, BIQI of 81.14 for letter "R" and 66.36 for letter "G"), which shows usefulness of the tik-dct deblurring step. However, tik-dct deblurring after WST did not improve image quality.

The resulting images are shown in Figs. 3 and 4. We can see that the enhancement algorithms improve the experimentally obtained images since the final reconstructions look cleaner (less noisy) and somewhat sharper. The proposed algorithm seems the most successful, especially in denoising.

5. CONCLUSION

We propose a complete imaging system, from experimental setup to image processing of the experimentally acquired images. The system uses a single MEMS mirror and a single photodetector to scan the image, thus ensuring low complexity, low power consumption, and small equipment size once

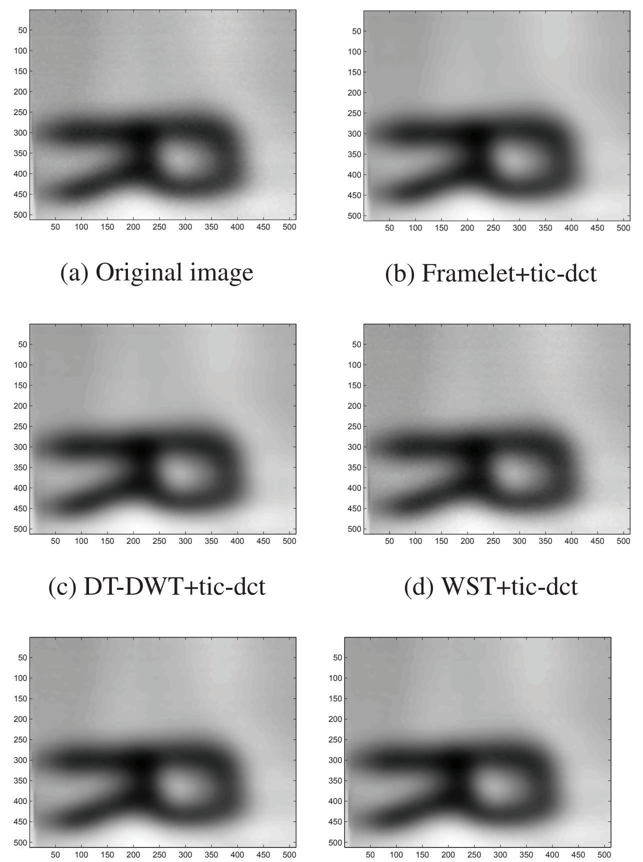

(a) Original image (b) Framelet+tic-dct

(c) DT-DWT+tic-dct (d) WST+tic-dct

(e) Proposed 1 itr (f) Proposed 2 itr

Fig. 3. Letter “R”: Visual quality comparison.

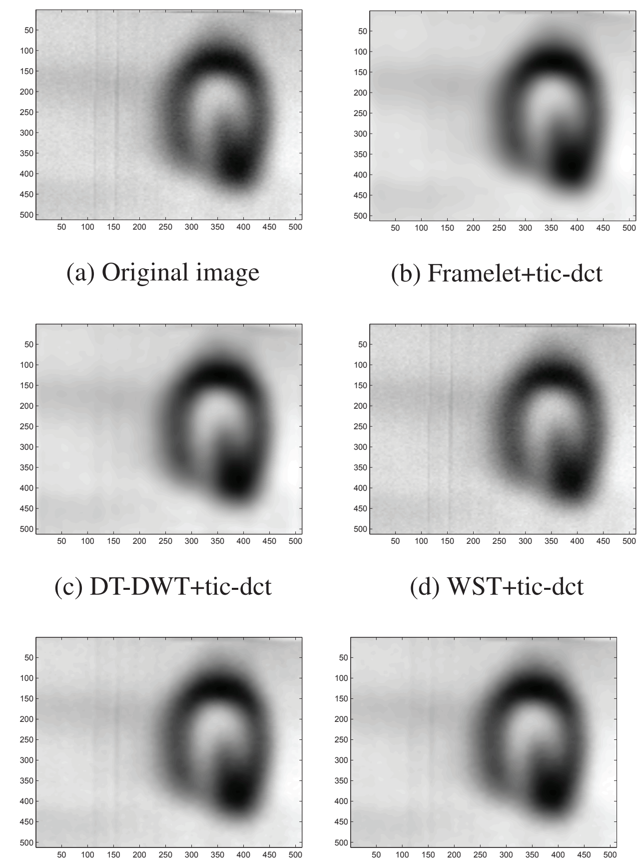

(a) Original image (b) Framelet+tic-dct

(c) DT-DWT+tic-dct (d) WST+tic-dct

(e) Proposed 1 itr (f) Proposed 2 itr

Fig. 4. Letter “G”: Visual quality comparison.

manufactured. The images acquired from the imaging hardware are significantly enhanced by customizing state-of-the-art algorithms to specific MEMS images. Objective and subjective results demonstrate impressive image quality improvement between enhanced images and the experimental outputs.

Due to the multidisciplinary nature of this work, future work to improve the overall system can go via two routes. One is improving the experimental setup, and the other is to better tailor denoising and deblurring steps into a single cohesive enhancement algorithm based on sparse representation.

6. REFERENCES

[1] L. Li, M. Mirza, V. Stanković, L. Li, L. Stanković, D. Uttamchandani, and S. Cheng, “Optical imaging with scanning MEMS mirror a single photodetector approach,” *ICIP-2009 IEEE Intl. Conf. Image Proc.*, Cairo, Egypt, Nov. 2009.

[2] M. Elad and M. Aharon, “Image denoising via sparse and redundant representations over learned dictionaries,” *IEEE Trans. Image Processing,* vol. 15, pp. 3736–3745, Dec. 2006.

[3] P. C. Hansen, J. G. Nagy, and D. P. O’Leary, *Deblurring Images - Matrices, Spectra, and Filtering,* SIAM, Philidelphia, 2006.

[4] A. Tikhonov and V. Arsenin, *Solution of Ill-Posed Problems,* New York: Wiley, 1977.

[5] J. Tropp and A.C. Gilbert, “Signal Recovery from Random Measurements via Orthogonal Matching Pursuit,” *IEEE Trans. Inform. Theory,* vol. 53, pp. 4655–4666, Dec. 2007.

[6] A. K. Moorthy and A.C. Bovik, “A two-step framework for constructing blind image quality indices,” *IEEE Sig. Proc. Letters,* vol. 17, pp. 513–516, May 2010.

[7] C. Liu, W.T. Freeman, R. Szeliski, S.B. Kang, “Noise estimation from a single image,” *CVPR-2006 IEEE Conf. Computer Vision and Pattern Recognition,* New York, NY, 2006.

[8] J. Mairal, F. Bach, J. Ponce, and G. Sapiro, “Online dictionary learning for sparse coding,” *Proc. the 26th Intl. Conf. Machine Learning,* Montreal, Canada, 2009.

[9] I. Daubechies, B. Han, A. Ron, and Z. Shen, “Framelets: MRA-based constructions of wavelet frames,” *Appl. Comput. Harmon. Anal.,* vol. 14, pp. 1–46, Jan. 2003.

[10] N. G. Kingsbury, “Complex wavelets for shift invariant analysis and filtering of signals,” *Appl. Comput. Harmon. Anal.,* vol. 10, pp. 234–253, May 2001.

[11] D. L. Donoho, “Denoising by soft-thresolding,” *IEEE Trans. Inform. Theory,* vol. 41, pp. 613-627, March 1995.

[12] D. Gunawan, “Denoising images using wavelet transform,” *Proc. IEEE Pacific Rim Conf. Commun, Computers and Sig. Proc.* pp. 83–85, 1999.